LAWRENCE
LIVERMORE
NATIONAL
LABORATORY

UCRL-JRNL-204382

High Volume, Low Pressure Drop, Bioaerosol Collector Using a Multi-slit Virtual Impactor

W. Bergman, J. Shinn, R. Lochner, S. Sawyer, F. Milanovich, R. Mariella Jr

May 27, 2004

Journal of Aerosol Science

Abstract

A bio-aerosol collector was developed comprising a low pressure drop, multi-slit virtual impactor, a wetted wall cyclone collector from Research International (RI), and associated plumbing and blower. The collector is portable, samples air at 1,220 L/min, provides 3-8 mL liquid sample, and has 70 W power consumption. The RI collector was selected for this unit following an evaluation of leading commercial aerosol collectors. The compact, multi-slit virtual impactor has an area of 334 cm^2 and a pressure drop of 0.2 kPa at an inlet flow of 1,220 L/min. The virtual impactor reported here concentrates the aerosols by a factor of four when the major to minor flow is adjusted to 4:1 ratio, but it has been field operated at a ratio of 8:1 when sampling at 2,300 L/min. This bio-aerosol collector has been incorporated in autonomous pathogen detection systems. This work was performed under the auspices of the U.S. Department of Energy by University of California, Lawrence Livermore National Laboratory under Contract W-7405-Eng-48.

1. Introduction

Lawrence Livermore National Laboratory (LLNL) has been developing technology for the U.S. government to address the threat of biological agents against civilian populations since 1996 (Milanovich, 1998). A key element of this program is the development of bio-detectors that can be used in the field by emergency response personnel. Such a device would have to be portable and provide results in less than one hour. The leading technology for the detectors are a miniature flow cytometer that uses an immunoassay analysis to detect proteins on the surface

of cells and a PCR (polymerase chain reaction) system to identify the DNA inside the cell (Milanovich, 1998). These analytical systems require a bio-aerosol collector that can rapidly collect sufficient airborne biological agents and inject them into a small water sample for subsequent analysis. A review of the common bio-aerosol collectors showed that a low power, portable, high sample volume collector with a small water sample was not available (Cox and Wathes 1995, Macher and Burge 2001, and Reponen et al 2001).

The reference bio-aerosol collector for biological warfare agents in the U.S. is the XM2, which was developed in the early 1990s by the U.S. military for use in the Biological Integrated Detection System (BIDS). The BIDS is a mobile biological laboratory used by the U.S. Army since 1996 for sampling and analyzing for biological agents . An important component of the BIDS is the XM2 aerosol collector, that is used for obtaining aerosol samples for subsequent analysis. The XM2 collector consists of three stages illustrated in Figure 1: a PM10 for removing particles larger than 10 μm, a virtual impactor for concentrating the aerosols, and a wetted wall collector for trapping the aerosols in a liquid. The particles suspended in the liquid, typically water, are analyzed in a subsequent analysis. The XM2 has been commercially available since the mid 1990s (SCP Dynamics, 7791 Elm St. NE, Minneapolis, MN 55432; Dycor, www.dycor.com) and is the conceptual design for the bio-aerosol collector in this study.

The objective of this study is the development of a portable, low power consumption, high volume aerosol collector that injects the particles in a small liquid volume, is smaller than 28 L (0.03 m^3) and can function either as an independent unit or be coupled directly to a detector. The biological aerosols are collected in a water reservoir for subsequent analysis. To improve the collection rate of the collector, a multi-slit virtual impactor is developed and used as an aerosol concentrator at the inlet of the wet collector. The objective of this study is to design and build a

portable, low power consumption collector based largely on the XM2 design, except for the PM10 inlet, which was deferred to a future study.

2. Evaluation of Commercial Collectors

The leading commercially available biological aerosol collectors are evaluated in this study to determine if they can be used in a high volume bio-aerosol collector. The collectors evaluated are the SASS 2000 RI unit (Research International, 17161 Beaton Road SE, Monroe, Washington 98272), SpinCon (Midwest Research Institute, 425 Volker Blvd,Kansas City, MO 64110), SCAEP unit (Team Technologies, 90 Oak Street, Newton Upper Falls, MA 02164), XM2 model SCP-1026 (SCP Dynamics, Inc, 7791 Elm St. NE, Minneapolis, MN 55432), and a glass impinger, model AGI-30 (Ace Glass,1430 Northwest Blvd., Vineland, NJ 08362). The XM2 collector is the current collector used in the U.S. military, and the AGI-30 is a frequently used reference collector in comparative tests.

The commercially available collectors are screened for collection efficiency using heterodisperse dioctyl sebacate (DOS) aerosols generated with a Laskin nozzle generator (Virtis, 815 Route 208, Gardiner, NY 12525) and an aerodynamic particle sizer (APS) (TSI, 500 Cardigan Road , Shoreview, MN 55126) to measure the aerosol size and concentration. Each of the collectors is connected to a source of constant aerosol concentration, and the aerosol concentration is measured at the inlet and the exhaust of the collector. Although this measurement determines the aerosol capture efficiency of the collector, it does not measure the collection efficiency in the liquid sample. Thus, the screening tests using the aerosol samples represent an upper limit efficiency of the collectors. The collection efficiency in the liquid sample will be less due to aerosol losses such as deposition on the collector walls.

The aerosol collection efficiency is determined from the aerosol concentration measurements in the inlet and exhaust of the collector using the following equation:

$$E = 100\ (1 - C_E / C_I) \qquad (1)$$

where E = aerosol capture efficiency, %

C_E = aerosol concentration in the exhaust

C_I = aerosol concentration in the inlet

The results of the efficiency measurements are shown in Figure 2, where the aerosol collection efficiency is plotted as a function of aerosol diameter. The collection efficiency of the collectors decreases in the following sequence: AGI-30> SPINCON> XM2> RI. The collection efficiency for the SCAEP collector could not be determined because the exhaust contained too many aerosols that were generated in the electrostatic spraying process. However, because of additional problems such as periodic electrical shorts that shuts down the collector, high power consumption (220 W), and excessive size (57 L) and weight (20 kg), no attempt was made to obtain alternative efficiency measurements on the SCAEP collector.

The collection efficiency also varies with the type of aerosols sampled as seen in Figure 3, where the collection efficiency of the RI collector is plotted as a function of particle size for DOS, AC Fine road dust (Powder Technology, Inc, 14331 Ewing Ave, South, Burnsville, MN 55337), and baker's yeast. Since the aerosol measurements are based on aerodynamic size, differences in density are already included in the size measurement. The road dust aerosol is generated using a TSI small scale powder disperser, model 3433 and neutralized with a TSI Kr-85 neutralizer, model 3054. The higher collection efficiency for the road dust is probably due to

the hygroscopic nature of the dust that causes an increase in particle size. The yeast aerosols are generated by creating a suspension of baker's yeast in water and nebulizing the suspension with a Wright nebulizer (Raabe, 1976). The yeast aerosols have comparable efficiencies to the DOS aerosols, which are hydrophobic and do not adsorb much water. This follows because the yeast aerosols are saturated with water since they are freshly generated from a water suspension.

The aerosol collection rate is a better measure of the various collectors than the efficiency because it provides a measure of the quantity of biological particles that are collected for subsequent analysis. The rate is determined by multiplying the collection efficiency by the sample flow rate. Figure 4 shows the resulting aerosol collection rates as a function of aerosol diameter for the four collectors. This figure clearly shows that the air sampling rate is the dominant factor determining the aerosol collection rate. The sequence of collectors arranged according to decreasing aerosol collection rate is XM2> SpinCon> RI> AGI-30.

However, to evaluate the aerosol collectors for the application as a portable, low power unit, the collection rates must be normalized to collector volume (or weight) and power consumption. The power consumption is computed from the current measurements using a clamp-on meter and the 110 V AC line voltage. The normalization is performed by dividing the collection rate by the collector volume or power consumption. Table 1 summarizes the values of key parameters of the collectors evaluated in this study. The AGI-30 collector has an external diaphragm pump included in the parameters for size, volume and weight. These parameter values are used to generate the collection rates normalized to collector volume and power consumption in Figures 5 and 6 respectively. As seen in these figures, the RI unit clearly stands out as the preferred commercial unit for integrating with the virtual impactor. The sequence of increasing normalized collection rates for both figures is RI> XM2>SpinCon> AGI-30.

2. Determination of sample flow rate for RI-LLNL collector

The sample flow rate of the RI collector is too low to collect a sufficient concentration of aerosols in the liquid sample for the selected analytical techniques. The required air flow rate for the collector is defined by

$$Q = \frac{C_D V_L F}{C_A (1-L)\, t} \qquad (2)$$

where Q = air flow rate, L/min

C_D = concentration detection limit in liquid, number agents/L

V_L = volume of liquid in collector, L

C_A = concentration of agents in air, number agents/L

t = air sample collection time, min

F = liquid sample dilution factor, greater or equal to 1

L = particle losses in the collector, fraction

Equation 2 shows that the flow rate is directly proportional to the volume of collected liquid and to the concentration detection limit of the analytical technique. Thus the smaller liquid volume and greater detector sensitivity (smaller C_D) favor smaller air sample flow rates.

The greatest factor affecting the required flow rate is the detection limit of the analysis method used. Belgrader et al. (1999a) used immunoassay methods and found $C_D = 10^6$ cfu/L

(colony forming units/liter) for the detection of bacterial spores of Bacillis subtilis var. niger (a simulant for anthrax) within five minutes. McBride et al (2003) used immunoassay methods and found C_D for Bacillus anthracis is 3×10^8 cfu/L and for Yersinia pestis is 6×10^6 cfu/L, both for a one minute analysis. Belgrader et al (1999b) used PCR (polymerase chain reaction) for nucleic-acid based analysis of Erwinia herbicola, a vegetative bacterium. They found they could measure 5 bacteria in a 5 μL sample that was diluted with 20 μL of PCR mix. This corresponds to a concentration of 10^6 bacteria/L in the sample. Belgrader et al (2003) also developed a flow-through PCR apparatus and showed they could detect less than 3 genomic DNA of Bacillis anthracis (B.a.) in a 2 μL sample that was diluted with 9 μL PCR mix within 30 minutes. This corresponds to a concentration of 1.5×10^6 B.a./L. Thus the C_D values range from 10^6 to 3×10^8 for immunoassay analysis in 1-5 minutes and from 10^6 to 1.5×10^6 for PCR analysis in 7-30 minutes.

The other parameters in Equation 2 have a much smaller effect on the required air flow. The most important of these is the liquid volume, where the required air flow is directly proportional to the liquid volume. The sample dilution factor takes into account any additional dilution of the sample by the reagents required in the sample preparation and analysis. For example if 20 μL of reagents are added to 5 μL of sample, then the dilution factor is 5. This parameter may be included in the detection limit. The particle loss term includes all losses that occur in the aerosol collection and in the liquid processing. In the tests using the RI collector, about 30% of the collected particles in the liquid sample hang up in the wet wall cyclone. It takes three collection cycles of clean sample to purge the residual particles from the RI collector. McBride et al (2003) and Langlois et al (2000) have observed these residual particles in their measurements

and the subsequent purging with clean samples. The three consecutive cycles of positive readings following a true positive provides confirmation of the measurement and could permit some rejection of narrow-time noise spikes. The loss in the aerosol sample is a function of particle size as shown in Figures 2 and 3. The loss from additional components of the collector such as aerosol pre-treatment devices are also included in the loss term.

The volume flow rate needed for a bio-aerosol collector is estimated for applications where the collector is used to detect biological agents such as anthrax. Assuming $C_D = 3 \times 10^8$ cfu/L for immunoassay analysis of Bacillus anthracis, $V_L = 8$ mL, F = 1, and L = 0.5, then $Q = 4.8 \times 10^6/C_A$ t. For a 30 minute sampling time per sample, the required flow rate is 160,000 L/min for C_A = 1 cfu/L and 1,600 L/min for C_A = 100 cfu/L. If PCR is used for analyzing B.a., then C_D is 10^6 and $Q = 16{,}000/ C_A$ t. Assuming a 30 minute sampling time per sample, the required flow rate is 533 L/min for C_A = 1 cfu/L and 5.3 L/min for C_A = 100 cfu/L. It is clear that the much higher sensitivity of the PCR analysis will allow much lower sample flow rates.

Peters and Hartley (2002) have estimated that the lethal dose for 10% of people, LD(10), exposed to anthrax aerosols is 50-98 spores based on an extrapolation from studies of monkey exposure, where the lethal dose for 50% of the monkeys is 4,100-8,000 spores. Considering that normal human breathing is about 10 L/min, a 1 minute exposure to a concentration of 10 cfu/L or a 10 minute exposure to a concentration of 1 cfu/L can result in inhaling 100 spores. Although extrapolations from monkey exposure to human exposure to anthrax aerosols is tenuous, these extrapolations suggest that a bio-collector that proposes to detect bio-agents such as anthrax must have sample flow rates of several thousands of liters per minute using immunoassy methods and

several hundreds of liters per minute using PCR methods. A detector that does not meet these requirements and only detects higher concentrations would still be useful in the "detect-to-treat" mode.

Of the aerosol collectors evaluated in this study, only the XM2 at 997 L/min in Table 1 came close to meeting the flow requirement. To use the RI collector in a detection system for measuring exposures to anthrax and other bio-agents, the sample air flow has to increase from 265 L/min to at least 1,600 L/min to allow detection of an average concentration of 100 cfu/L over a 30 minute sampling period when using immunoassy detection methods. If a cloud of bio-agents is transient, then the peak concentration will have to be much higher than 100 cfu/L to provide a detectable measurement.

To develop a portable bio-aerosol collector, the concepts in the commercial XM2 collector are adopted whereby two stages of virtual impactors are used to concentrate the ambient aerosols from about 1,000 L/min to 20 L/min for collection in a wet collector (Kesavan and Doherty 2001). The first stage virtual impactor in the XM2 consists of multiple opposing jets to concentrate the particles from an air flow of 1,000 L/min to 100 L/min (Kesavan and Doherty 2001). Marple and Liu (1987) and Marple et al (1990) have developed the use of opposing jets for concentrating aerosols. A second stage virtual impactor, consisting of single opposing slits further concentrate the aerosols from 100 L/min to 20 L/min (Kesavan and Doherty 2001).

Although the XM2 collector also has a PM10 inlet separator that consists of a tortuous path to reject particles larger than 10 μm, that component is not included in the RI-LLNL collector due to budget constraints. This important component will be added in the future.

3. Development of multi-slit virtual impactor

The virtual impactor to be used in the bio-aerosol sampler has to have a low pressure drop in order to use a low power consumption blower. Marple and Liu (Marple and Liu 1987, Marple et al 1990) showed that multiple nozzles significantly reduce the pressure drop for a given flow rate and particle size cut point. They showed that the pressure drop is proportional to $n^{-2/3}$, where n is the number of nozzles.

Romay et al (2002) applied these principles to develop an aerosol concentrator for biological agent detection. They developed a two stage virtual impactor with 40 nozzles in the first stage to concentrate 300 L/min into 15 L/min output to the second stage. The second stage processed 15 L/min into 1 L/min output. Romay et al (2002) experimentally measured the combined concentration increase for different particle sizes and ranged from 99 at 2.05 μm to 293 at 3.94 μm and 231 at 8.51 μm. These results show modest particle losses compared to the theoretical factor of 300 for no particle losses.

However, the pressure drop across the virtual impactor is 2.0 kPa for the first stage and 3.5 kPa for the second stage. These pressure drops are far too high for a low power consumption biocollector. To achieve a pressure drop of less than 0.2 kPa at a flow of 1,200 L/min, a virtual impactor with 186 nozzles is needed according to Marple's formula. However, such a design would not likely result in a low cost virtual impactor because of the difficulty in aligning two sets of 186 nozzels.

To address this deficiency, a virtual impactor is developed based on a multi-slit design using the basic design criteria described by Marple and Chien (1980) and Marple et al (2001) for cylindrical nozzle designs. Other researchers have previously developed single slit virtual impactors (Sioutas et al 1994). The principle of the multi-slit virtual impactor is illustrated in

Figure 7 (Bergman et al 1999, Bergman 2002). A perspective drawing of the multi-slit virtual impactor is shown in Figure 8, and the key design parameters are given in Table 2.

The particle laden air enters from the top and is accelerated in the funnel section into the accelerator slits as shown in Figure 7. Particles are forced into the collector slits due to their inertia and penetrate to the bottom of the impactor with the minor flow. The major air flow is deflected around the collector slits and into the more open exhaust channels. The major flow is pulled out at right angles through both ends of the virtual impactor. An end plate, partially shown in Figure 8, covers the top portion of the major flow channels to promote the downward air flow prior to exiting the impactor as the major flow. The end plate also serves to seal the ends of the collector slits. Figure 9 shows a composite of two superimposed photographs of the virtual impactor, with and without the end plate installed. Two rods pass through the collector slits for alignment and rigidity. Separation between the two plates defining each collector slit is maintained by dimples impressed on one of the plates.

Although there are no restrictions on the number of slits that can be used in a virtual impactor, there is a restriction on the length of the slits. Since most of the inlet air to the impactor is pulled out through the ends as the major flow, there is an unavoidable increase in the inlet air velocity near both ends of the impactor. This uneven distribution of air velocity into the virtual impactor is mitigated by restricting the length of the slits. Thus the virtual impactor element is designed to limit the slit length to 9.14 cm and is arbitrarily chosen to be a square. A photograph of the final virtual impactor consisting of four multi-slit sections, each 9.14 cm by 9.14 cm, is shown in Figure 10. The spaces between adjacent multi-slit sections act as manifolds for the major air to be exhausted. The key features of the multi-slit virtual impactor are its small size

relative to the air flow, the simplicity of its design and construction, and the very low pressure drop.

A preliminary evaluation of the multi-slit virtual impactor is conducted using monodisperse DOS aerosols tagged with sodium fluorescene (SF). Monodisperse particles having diameters of 5.1, 5.4, 7.4, and 14.7 μm are generated using various concentrations of DOS/SF in ethanol in a TSI vibrating orifice generator, model 3450 (TSI, 500 Cardigan Road , Shoreview, MN 55126). The experiment consists of injecting the DOS/SF aerosols into the top portion of the vertical test duct and thoroughly mixing with HEPA filtered air to produce 1,220 L/min flow through the multi-slit virtual impactor. The impactor is mounted at the bottom of the rectangular duct and is sealed around the circumference of the impactor. A push-pull flow system is used to avoid creating a negative pressure at the collector inlet because of the resistance from the HEPA filter and the Meriam laminar flow meter, model 50MC2-4 (Meriam Instrument, Cleveland, OH 44102). One blower upstream of the HEPA filter provides the push, while a second blower downstream of the virtual impactor provides the pull. The downstream blower is used to pull both the major flow of 995 L/min and the minor flow of 265 L/min. Restrictions in the major and minor flow paths are calibrated separately to control the two flow rates.

The impactor is operated for about 10 minutes, after which it is disassembled and rinsed with alcohol to remove any DOS/SF deposits. The rinses from the top plate, the multiple plates defining the receiving slits, and the bottom plate are analyzed for SF and compared to the total SF entering the impactor. To determine the total SF entering the virtual impactor, a HEPA filter paper is placed over the inlet of the impactor; and, following the exposure, the deposits are rinsed off. Separate tests are conducted for each aerosol size.

The rinses from the DOS/SF tests are analyzed and converted to percent of SF lost in the impactor for each of the impactor components and the total and are given in Table 3. Except for the 14.7 μm aerosol, the multi-slit virtual impactor typically has less than 15% particle loss.

4. Integration of multi-slit virtual impactor with RI collector

Based on the evaluation of the commercial collectors, the RI collector was selected for use in the low power consumption, portable collector. A contract was issued to Research International to attach the multi-slit virtual impactor to the inlet of their unit.

The cross section drawing of the RI collector is shown in Figure 11. Air enters at the bottom into a cyclone where a water spray is added to mix with the incoming air. The circling air and water drops then pass though a wetted column that collects the water drops. Any water that flows up the column with the air flow is collected in a circumferential water trap and is recycled or pumped to a sample vial. An air blower (not shown) is installed on the top of the demisting (cistern) section to provide the air flow.

Research International built the integrated collector containing the multi-slit virtual impactor and the RI collector shown in Figure 12. The unit is 43 cm x 25 cm x 34 cm. Sample air enters the virtual impactor from the top, and the minor flow exits from the bottom through a funnel and a tube to the inlet of the RI collector (not shown). The blower that is part of the RI collector is used to pull 265 L/min from the minor flow of the impactor through the RI collector. A separate blower is added to the integrated unit to remove the major flow of 955 L/min from the virtual impactor. Although the preferred design for the impactor exhaust is a manifold around the perimeter of the impactor with a connecting pipe to the exhaust blower, the alternative design shown in Figure 12 was selected for expediency. The selected design consists of placing the

virtual impactor and RI collector in a leak-free, sealing box and applying a vacuum to the box with the exhaust blower. The disadvantages of this approach are the added requirement of a leak-tight box and aerosol contamination of all the components within the box.

5. Evaluation of RI-LLNL collector

The aerosol collection efficiency of the RI-LLNL collector is determined using several different aerosols and different detection methods. The total inlet flow rate of 1,220 L/min is measured directly with the Meriam laminar flow element. The major flows from the virtual impactor (housing exhaust flow) and the exhaust flow from the RI collector are measured using hot wire anemometers placed in the respective exit pipes. The exhaust flow from the RI collector is also the minor flow from the multi-slit virtual impactor since the exit of the virtual impactor connects directly to the inlet of the RI collector. Converting the hot wire velocity measurements to flows yield 905 and 315 L/min for the exhaust and sample flows respectively. Thus, the virtual impactor samples 315/1220 or 25% of the total flow; or, alternatively, the aerosol concentration is increased by a factor of 4. Pressure tap measurements in the tube leading from the virtual impactor to the RI collector show a pressure of 0.07 kPa. The pressure in the sealing box is 0.2 kPa. These measurements show that a flow of 1,220 L/min into the virtual impactor splits into a sample flow of 315 L/min with a resistance of 0.07 kPa and an exhaust flow of 905 L/min with a resistance of 0.2 kPa. In alternative designs using a single blower, restrictions must be placed in the sample flow to equalize the pressure in both flows. The total power usage for the RI-LLNL collector is about 70 watts, most of which is due to the blower pulling the major air flow from the virtual impactor.

The efficiency of the RI-LLNL collector is determined using measurements in the collected liquid as well as in the air streams. The efficiency measurements from aerosol measurements provide the maximum potential efficiency if there are no losses in the collector or connecting tubing. These measurements are made with heterodisperse DOS and monodisperse latex aerosols using the procedure previously described. The additional liquid measurements are important because they represent the actual efficiency of collecting particles that are available for subsequent detection and analysis.

The technique used for determining the particle collection efficiency in the liquid sample is to use latex particles and a flow cytometer detector. In these tests, an AGI-30 collector is modified to replace the right angle inlet tube with an isokinetic inlet probe directed vertical into the air stream. The modified AGI-30 collector is suspended inside the vertical duct to provide the measurement of the challenge aerosol in a liquid sample. The AGI-30 is frequently used as the reference collector because of the nearly quantitative collection for particles greater than 0.5 μm as seen in Figure 2. The particle collection efficiency in this test is determined from the fraction of particles collected in the RI-LLNL liquid sample to the particles collected in the AGI-30, both measurements corrected for the corresponding flow rates. Since the AGI-30 only samples 12 L/min compared to the 1220 L/min for the RI-LLNL collector, the number of particles in the AGI-30 are multiplied by 100 for the comparison.

Initially, 1.88 μm unlabeled latex aerosols were used in these tests, but the latex particles could not be resolved from background debris in the AGI-30 liquid sample. The background debris probably results from the emulsifier contained in the liquid latex sample. Because of the much greater air flow, the RI-LLNL collector sample has sufficient latex particles above background to provide a good measurement. However, the few particles collected in the AGI-30

samples were indistinguishable from the background. To resolve the problem with the background debris in the AGI-30 sampler, fluorescent labeled 2.0 μm latex were used in subsequent tests. Both unlabeled and labeled latex samples are measured using a flow cytometer (Mariella Jr. et al 1999). Since the unlabeled latex concentration can not be determined in the AGI-30 sample, only the tests using labeled latex are used for determining the efficiency of the RI-LLNL collector based on liquid samples. These liquid measurements show the collection efficiency of the RI-LLNL collector is 57% for labeled 2.0 μm latex aerosols.

An important finding of the liquid particle measurements is the hang-up of particles in the collector. After removing the 3 mL sample, fresh water is added and the unit operated for about five minutes. This second sample is removed and a third charge of fresh water is added and operated for five minutes. Each of the three samples are analyzed for latex particles. The analysis shows that the first three samples contain 64.5%, 33% and 2.5% of the total particles counted respectively. Thus there is considerable hang-up of particles in the RI collector and should be considered when correcting for particle loss and for cross-contamination of sequential samples.

Collector efficiency tests are also conducted using heterodisperse DOS and 1.88 μm latex aerosols and the aerodynamic particle sizer (APS). The procedure is similar to that described in the section on evaluating commercial collectors. However, because there are one intake and two exhaust paths for the RI-LLNL collector (one from the virtual impactor exhaust and a second from the RI exhaust), separate measurements of the aerosol concentration and the flow rates of each of the three paths must be taken to compute collector efficiency. The efficiency is determined from Equation 3:

$$E = 100 \{1 - [V_{RI} C_{RI} + V_{IE} C_{IE}] / [V_I C_I] \} \qquad (3)$$

where E = aerosol capture efficiency, %

C = aerosol concentration

V = air flow rate

RI = measurement at the exhaust of the RI unit

IE = measurement at the exhaust of the virtual impactor

I = measurement at the inlet of the virtual impactor

Equation 3 and the DOS and latex concentration measurements are used for determining the filter efficiency for the RI-LLNL collector. The results are shown in Figure 13 along with the efficiency curve for the RI collector from Figure 2.

Figure 13 shows that the DOS collection efficiency for the RI-LLNL collector is only slightly lower than the comparable efficiency for the RI collector alone. Although the RI-LLNL collector uses only 3 mL of water in the wetted cyclone compared to 8 mL in the RI collector test, the lower efficiency is primarily due to the aerosol losses in the virtual impactor and associated tubing. The aerosol test on the RI-LLNL collector using 1.88 μm latex shows an efficiency of 57%, which is comparable to the DOS efficiency measurements on the RI collector but is 12% higher than the DOS efficiency measurements on the RI-LLNL collector. Since latex spheres are more hydrophilic than the DOS aerosols, this may explain some of the higher efficiency obtained with the latex aerosols compared to the DOS aerosols. The effect of material properties on collection was previously seen in Figure 3 where hydrophilic aerosols such as road dust have a higher collection efficiency than hydrophobic DOS aerosols. However, small differences in the efficiency measurements (i.e. +/- 5%) are generally due to experimental variability.

Another finding seen in Figure 13 is that the efficiency determined from the labeled latex particles collected in the liquid sample is comparable to the efficiency determined from DOS aerosol samples. The RI-LLNL collection efficiency of latex spheres in the liquid sample is 57% compared to 50% for the collection efficiency of DOS aerosols in the air sample. The 57% efficiency represents the total number of spheres measured in the sample plus the residues from two additional rinses. For comparison, the RI collector has an efficiency of 62% for DOS aerosols. Since the variability of the efficiency measurements is estimated at +/- 5% , these measurements are not significantly different.

Since the rate of aerosol collection is the critical parameter in evaluating collector performance, the efficiency measurements in Figure 13 are converted to the collection rates in Figure 14. This is done by multiplying the collector efficiencies in Figure 13 by the corresponding sample flow rates and the aerosol concentration (assumed 1 particle/L). The results in Figure 14 show that the aerosol collection rate of the RI-LLNL collector is about four times that of the RI collector alone. This increased collection rate is due to the virtual impactor, that effectively concentrates the larger aerosols into a smaller air flow.

To assess the performance of the RI-LLNL collector relative to the XM2 collector, which is the current reference collector, the collection rates of the two collectors are plotted in Figure 15. This figure shows that the XM2 has a significantly higher collection rate for aerosols below 3 µm. Above 3 µm, the two collectors have similar collection rates. However, the XM2 is much larger and requires much more power than the RI-LNL collector. In summary, the portability and the low power consumption of the RI-LLNL collector more than compensate for the lower collection rate at the smaller aerosol sizes.

Since the bio-aerosol collector described in this report was first completed in 1999 (Bergman et al 1999), the unit has been repackaged into a smaller size (approximately a 30 cm cube) as shown in Figure 16. A manifold is also added to the virtual impactor to exhaust the major flow through a tube rather than in an evacuated chamber. This modification, which is the original design based on the XM2, prevents ambient aerosols from contaminating the interior of the collector components. A more powerful blower is added to the collector to increase the sample flow rate to 2,300 L/min (McBride et al 2003). Another change is the addition of a particle counter to measure the ambient particle concentration. This is a common feature in collectors that do not operate continuously, but are turned on when a preset ambient concentration triggers the collector. The particle counter is not needed for continuous sampling. A rain cap is also added to the inlet of the virtual impactor to prevent rain and large objects (but not large particles) from being pulled into the collector as shown in Figure 17. The improved collector in has been evaluated in field tests (Langlois et al 2000, McBride at al 2003) and a number of units have been built and deployed in limited applications for monitoring for bio-agents. When the PM10 inlet for removing particles larger than 10 μm is added in the future, the portable collector will have all of the major design concepts from the XM2 shown in Figure 1.

6. Summary and Conclusions

A high volume, low pressure drop bio-aerosol collector is developed that is portable and has low power consumption. The collector design is based on the commercially available XM2 collector, which is the standard collector for biological warfare agents. The collector described in this report samples air at 1,220 L/min and has a flow resistance of 0.2 kPa. The bio-aerosol

collector consists of a multi-slit virtual impactor, a wetted-wall cyclone collector from Research International, a blower and associated plumbing and controls.

The Research International collector was selected from an evaluation of leading commercial collectors based on high sample volume (365 L/min), low power consumption (13.8 W), and small volume of collected water (3-8 mL). Efficiency tests using DOS aerosols show an increasing efficiency with particle size from 22% at 1.0 μm to 50% at 1.75 μm and to 90% at 3.0 μm. Other aerosols such as latex spheres and yeast cells show comparable efficiencies, while Arizona road dust has higher efficiency presumably due to water adsorption.

The multi-slit virtual impactor consists of 4 modules, 9.1 cm square and 2.5 cm thick packaged into a 23 cm square and 2.5 cm thick unit. Each of the modules have 21 virtual impactor slits that are 4.24 mm apart. The effective open area of the virtual impactor is 11.8 %, which represents the relative area of the accelerating slits compared to the total area. The high density of the slits is responsible for the low flow resistance of the multi-slit virtual impactor. At 1,220 L/min flow, the pressure drop across the virtual impactor is 0.2 kPa. Tests using fluorescene labeled DOS aerosols show that there is about 5% particle loss in the virtual impactor between 5-7 mm.

The RI wet wall cyclone and the multi-slit virtual impactor are integrated to create the RI-LLNL collector, in which the minor flow from the virtual impactor enters the RI collector. The RI-LLNL collector samples 1,220 L/min and has a power consumption of about 70 W. Aerosol collection efficiency measurements are made using DOS aerosols and latex spheres by measuring the aerosol concentration entering the exiting the collector. The collection efficiency with DOS aerosols is 22% at 1.0 μm, 50% at 2.0 μm, and 77% at 3.0 μm diameter. These collection efficiencies are slightly less than that for the RI unit alone because of particle loss in

the virtual impactor. The efficiency using 1.88 μm latex sphere diameter in aerosol measurements is 57%. A separate test using fluorescently labeled latex spheres and measuring the quantity of spheres in the liquid sample show the collection efficiency for 2 μm spheres is 57%. The liquid sample confirms that the efficiency measurements with aerosols are an approximate assessment of the collector efficiency.

The collector described in this report has been repackaged into a smaller size and incorporated into autonomous pathogen detection systems (Langlois et al 2000, McBride et al 2003). These detection systems are large units, about the size of an automated teller machine, and are not portable. Future efforts are aimed at reducing the size and portability of these pathogen detection systems, including the aerosol collector described here.

References

Belgrader,P., Bennett, W., Bergman, W., Langlois, R., Mariella Jr., R., Milanovich, F. Miles, R., Venkateswaran, K., Long, G., and Nelson, W. (1999a) Autonomous system for pathogen detection and identification, *SPIE Proceedings* **3533**, 198-206.

Belgrader, P., Benett, W., Hadley, D., Richards, J., Stratton, P., Mariella Jr., R., and Milanovich, F. (1999b) PCR detection of bacteria in seven minutes. *Science* **284**, Issue 5413, 449-450.

Belgrader, P., Elkin, C.J., Brown, S.B., Nasarabadi, S.N., Langlois, R.G., Milanovich, F.P., and Colston Jr., B.W. (2003) A reusable flow-through plymerase chain reaction instrument for the continuous monitoring of infectious biological agents. *Anal. Chem.* **75**, 3446-3450.

Bergman, W., Shinn, J., Lochner, R., and Sawyer, S. (1999) RI-LLNL hybrid biological aerosol collector, Lawrence Livermore National Laboratory , UCRL-ID-35282, http://www.llnl.gov/library/ .

Bergman, W. (2002) United States Patent, US 6,402,817 B1, Low pressure drop, multi-slit virtual impactor.

Cox, CS and Wathes, CM, (1995) *Bioaerosols Handbook* . Lewis Publishers, Boca Raton.

Kesavan, J and Doherty, R.W. (2001) Characterization of the SCP 1021 Aerosol Sampler, Edgewood Chemical Biological Center Report ECBC-TY-211, Aberdeen Proving Ground, MD. Available from National Technical Information Service, 5285 Port Royal Road, Springfield, VA 22161, report ADA397460, www.ntis.gov.

Langlois, R.G., Brown, S., Colston, B., Jones, L., Masquelier, D., Meyer, P., McBride, M., Nasarabadi, S., Ramponi, A.J., Venkateswaran, K., and Milanovich, F. (2000) Development of an autonomous pathogen detection system. In *Proceedings of the First Joint Conference on Point Detection*, Wlliamsberg, VA, Oct 23-27, 2000. http://www.llnl.gov/tid/lof/documents/pdf/238720.pdf.

Macher, J.M. and Burge, H.A. (2001) Sampling biological aerosols. In *Air Sampling Instrument, 9th Edition*, (Edited by Cohen, B.S. and McCammon Jr.,C.S.), pp. 661-701. American Conference of Governmental Industrial Hygienists, Cincinnati, www.acgih.org/store.

Mariella Jr.,R.P., Huang, Z., and Langlois, R.G. (1999) Characterization of the sensitivity of side scatter in a flow-stream waveguide flow cytometer. *Cytometry* **37**, 160-163.

Marple, V.A. and Chien, C.M. (1980) Virtual impactors: A theoretical study. *Environ. Sci Technol.* **14**, 975-985.

Marple, V.A. and Liu, B.Y.H. (1987) United States Patent, US 4,670,135 High volume virtual impactor.

Marple, V.A., Liu, B.Y.H, and Burton, R.M. (1990). High-Volume Impactor for Sampling Fine and Coarse Particles. *J. Air Waste Manage. Assoc.* **40**, 762-767.

Marple, V.A. and Liu, B.Y.H. (1991) United States Patent, US 5,040,424 High volume PM10 sampling inlet

Marple, V.A., Olson, B.A., and Rubow, K.L. (2001) Inertial, Gravitational, Centrifugal, and Thermal Collection Techniques. In *Aerosol Measurement, Priinciples, Techniques, and Applications, Second Edition* (Baron, P.A. and Willeke, K, Editors), pp. 229-260. Wiley-Interscience, New York.

Milanovich, F.(1998) Reducing the threat of biological weapons, LLNL's *Science & Technology Review*, Lawrence Livermore National Laboratory, June, http://www.llnl.gov/str/Milan.html

McBride, M.T., Masquelier, D., Hindson, B.J., Makarewicz, A.J., Brown, S., Burris, K., Metz, T., Langlois, R.G., Tsang, K.W., Byron, R., Anderson, D.A., Venkateswaran, K.S., Milanovich, F.P., and Colston Jr., B.W. (2003). Autonomous detection of aerosolized Bacillus anthracis and Yersinia pestis, *Anal.Chem*., **75**, 5293-5299.

Peters, C.J. and Hartley, D.M. (2002) Anthrax inhalation and lethal human infection. *Lancet*, **359**, 710.

Rabbe, OG. (1976) The generation of aerosols of fine particles. In *Fine Particles, Aerosol Generation, Measurement, Sampling, and Analysis* (Liu, B.Y.H. Editor), pp. 57-110. Academic Press, Inc., New York.

Reponen, T., Willeke, K., and Grinshpun, S., (2001) Biological particle sampling. In *Aerosol Measurement, Priinciples, Techniques, and Applications, Second Edition* (Baron, P.A. and Willeke, K, Editors), pp. 751-777, Wiley-Interscience, New York.

Romay, F.J., Roberts, D.L, Marple, V.A., Liu, B.Y.H., and Oslon, B.A. (2002) A High-performance aerosol concentrator for biological agent detection, *Aerosol Sci. and Tech*.,**36**, 217-226.

Sioutas, C., Koutrakis, P. and Burton, R.M. (1994) Development of a low cutpoint slit virtual impactor for sampling ambient fine aerosols. *J. Aerosol Sci.* **24**, 1321-1330.

Tables

Table 1. Characteristics of commercially available collectors

Unit	Flow (L/min)	Weight (kg)	Volume (L)	Power (W)[1]
RI[2]	265	3	14	13.8[3]
XM2	997	41	180	360
SCAEP	360	20	57	220
SpinCon	367	27	120	495
AGI-30 [4]	12	4	14	495

[1] All power measurements are made with line voltage.

[2] The liquid level is set to 8 mL.

[3] RI literature states 7.2 W when battery is used.

[4] A vacuum diaphragm pump is included with the AGI-30 to allow comparisons with the other collectors.

Table 2. Design parameters for multi-slit virtual impactor.

Parameter	Value
Accelerator slit height	2.64 mm
Accelerator slit width	0.508 mm
Accelerator slit length	91.4 mm
Accelerator inlet funnel angle	45°
Collector slit height	22.1 mm
Collector slit width	0.762 mm
Collector slit length	91.4 mm
Accelerator to Collector slit separation	1.52 mm
Slit to Slit Centers	4.24 mm
Number of slits per section	21
Number of sections per impactor	4

Table 3. Percent of aerosol lost in components of multi-slit virtual impactor

Component	Aerosol diameter, μm			
	5.1 μm	5.4 μm	7.4 μm	14.7 μm
Accelerating slits	2.6%	9.9%	3.4%	17.7%
Collector slits	0.7%	4.6%	0.2%	18.6%
Bottom plate	0.6%	0.3%	1.9%	0.5%
Total	3.9%	14.8%	5.5%	36.8%

Figure Legends

Figure 1. Conceptual design of the commercially available XM2 aerosol collector that consists of a PM10 inlet to remove particles greater than 10 μm, a virtual impactor to concentrate the collected aerosols, and a wetted wall collector to trap the particles in a liquid.

Figure 2. Aerosol collection efficiency of commercially available aerosol collectors as a function of aerosol diameter. The efficiency is determined using DOS aerosols measured entering and exiting the collectors.

Figure 3. Collection efficiency of DOS, road dust, and yeast for the RI collector as a function of the aerosol diameter.

Figure 4. Aerosol collection rate for commercially available aerosol collectors as a function of aerosol diameter. The curves are generated by multiplying the data in Figure 1 by the corresponding sample flow rates.

Figure 5. Aerosol collection rate for commercial collectors normalized to collector volume as a function of aerosol diameter. The curves are generated by dividing the data in Figure 4 by the corresponding collector volumes.

Figure 6. Aerosol collection rate for commercial collectors normalized to power consumption as a function of aerosol diameter. The curves are generated by dividing the data in Figure 3 by the corresponding collector power consumption.

Figure 7. Schematic showing a multi-slit virtual impactor. The air in the accelerating slits forces particles into the collector slits due to particle inertia while the major air flow is defected.

Figure 8. Perspective drawing of the multi-slit, virtual impactor.

Figure 9. Superimposed photographs showing the virtual impactor with the end plate installed and removed to show the parallel collector slits for the minor air flow and aerosols and the openings for the major air flow.

Figure 10. Photograph of the multi-slit virtual impactor that consists of four 9.1 cm x 9.1 cm segments assembled together. This photograph shows the top, multi-slit accelerating inlet and the major flow channels in the end plates. The minor flow exits from the bottom.

Figure 11. Schematic of RI wetted-wall cyclone bioaerosol collector.

Figure 12. Photograph of assembled RI-LLNL collector with virtual impactor inlet showing.

Figure 13. Collection efficiency of RI and RI-LLNL collectors for DOS and latex aerosols as a function of aerosol diameter.

Figure 14 Aerosol collection rate for DOS and latex aerosols in the RI and RI-LLNL collectors as a function of aerosol diameter.

Figure 15. Comparison of aerosol collection rates of the RI-LLNL collector to the XM2 collector. Collector flow rate, size and power consumption are shown in parenthesis.

Figure 16. Photograph of repackaged RI-LLNL collector with added optical particle counter. The ruler is 12 inches (30 cm).

Figure 17. Photograph of repackaged RI-LLNL collector with added optical particle counter and rain cap. The ruler is 12 inches (30 cm).

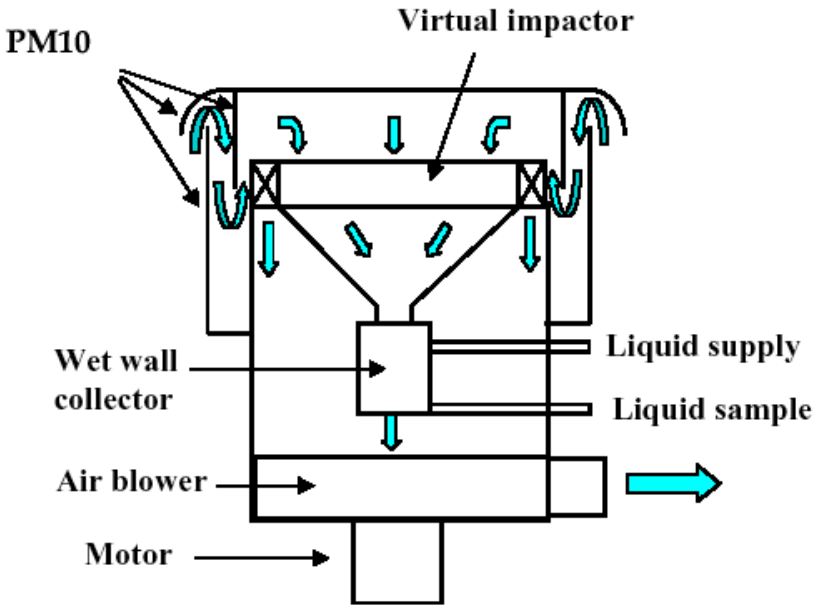
PM10
Virtual impactor
Wet wall
collector
Liquid supply
Liquid sample
Air blower
Motor

Figure 1

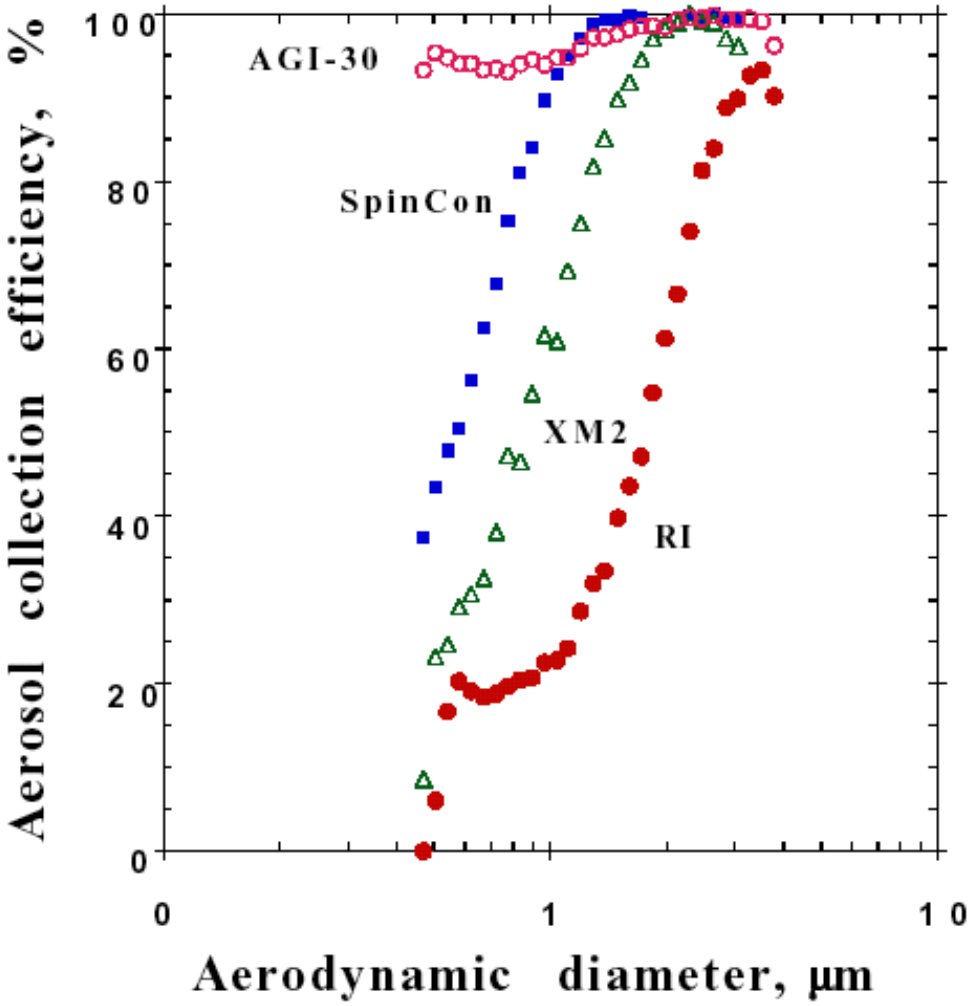
Aerosol collection efficiency, %
100
80
60
40
20
0
AGI-30
SpinCon
XM2
RI
0
1
10
Aerodynamic diameter, µm

Figure 2

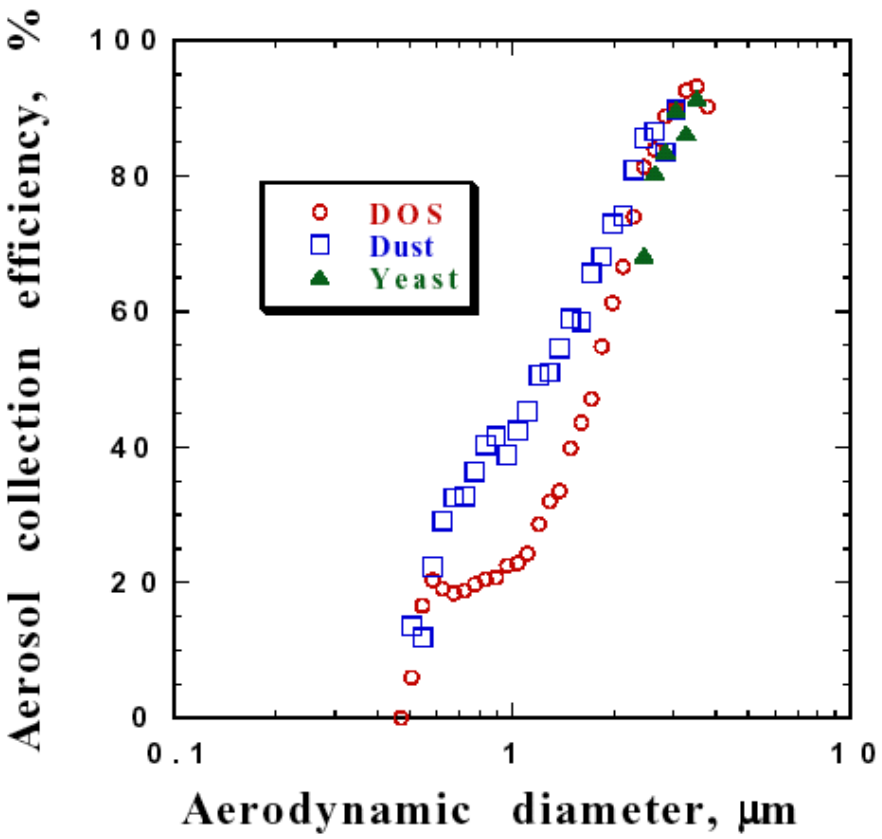
Aerosol collection efficiency, %
100
80
60
40
20
0
0.1
1
10
Aerodynamic diameter, µm
DOS
Dust
Yeast

Figure 3

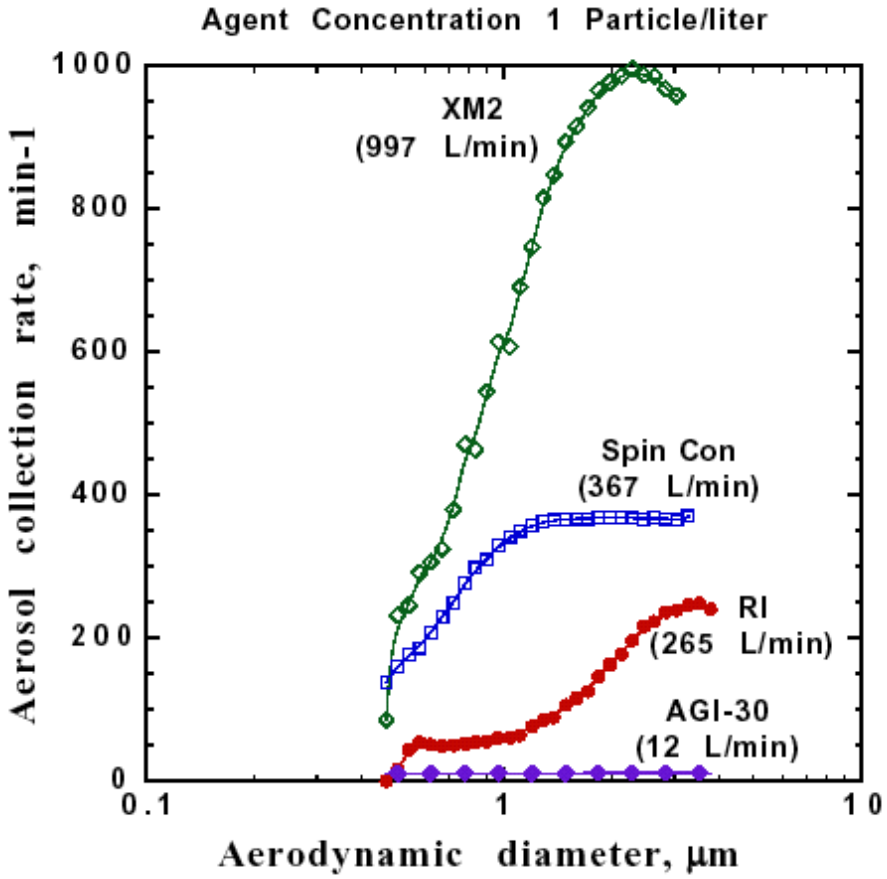
Agent Concentration 1 Particle/liter
Aerosol collection rate, min-1
1000
800
600
400
200
0
0.1
1
10
Aerodynamic diameter, µm
XM2
(997 L/min)
Spin Con
(367 L/min)
RI
(265 L/min)
AGI-30
(12 L/min)

Figure 4.

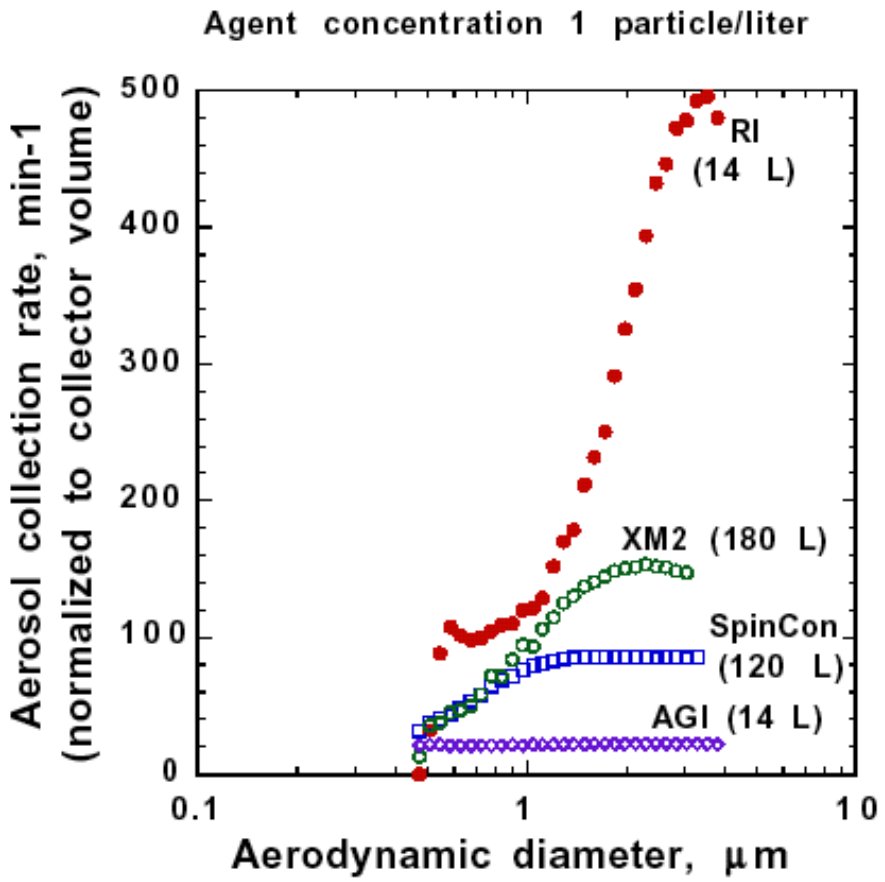
Agent concentration 1 particle/liter
Aerosol collection rate, min-1
(normalized to collector volume)
500
400
300
200
100
0
0.1
1
10
Aerodynamic diameter, µm
RI
(14 L)
XM2 (180 L)
SpinCon
(120 L)
AGI (14 L)

Figure 5

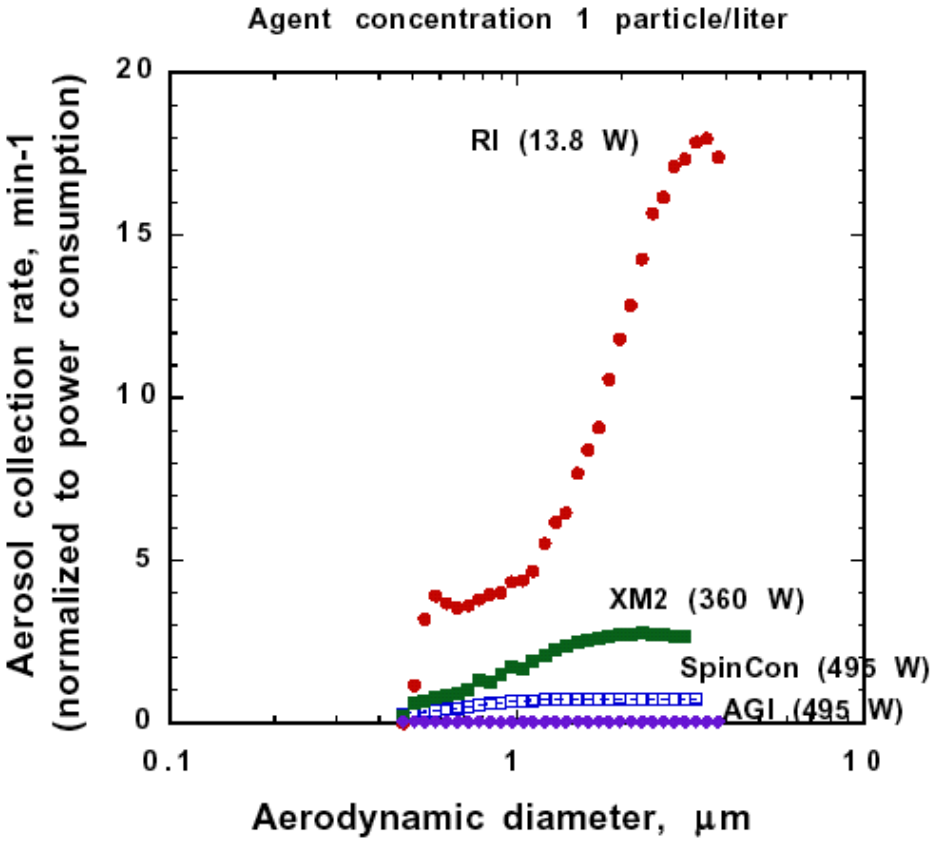
Agent concentration 1 particle/liter
Aerosol collection rate, min-1
(normalized to power consumption)
20
15
10
5
0
0.1
1
10
RI (13.8 W)
XM2 (360 W)
SpinCon (495 W)
AGI (495 W)
Aerodynamic diameter, µm

Figure 6

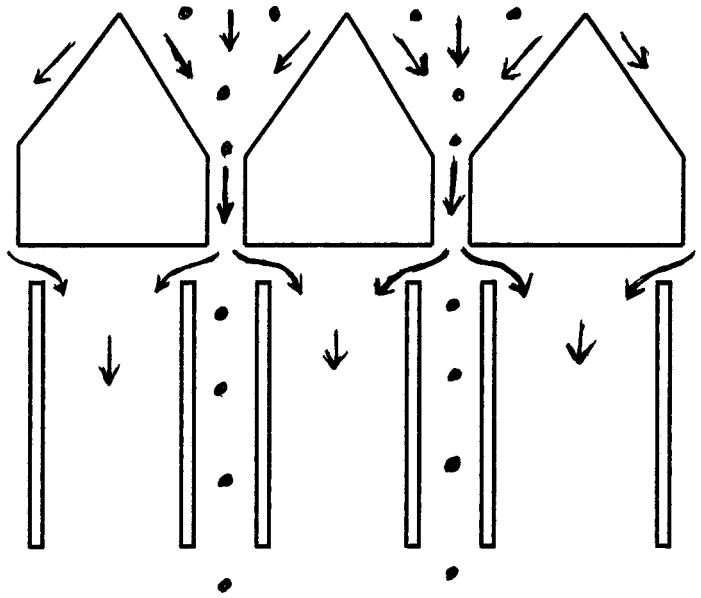

Figure 7

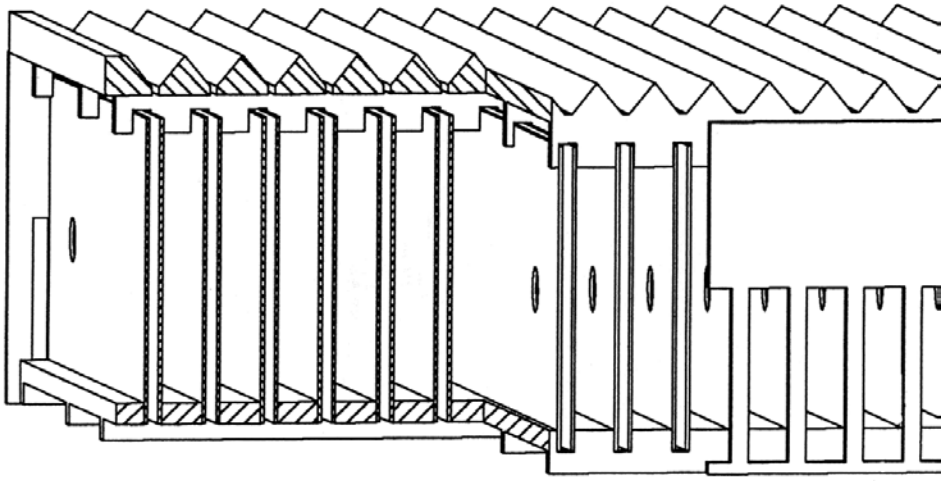

Figure 8

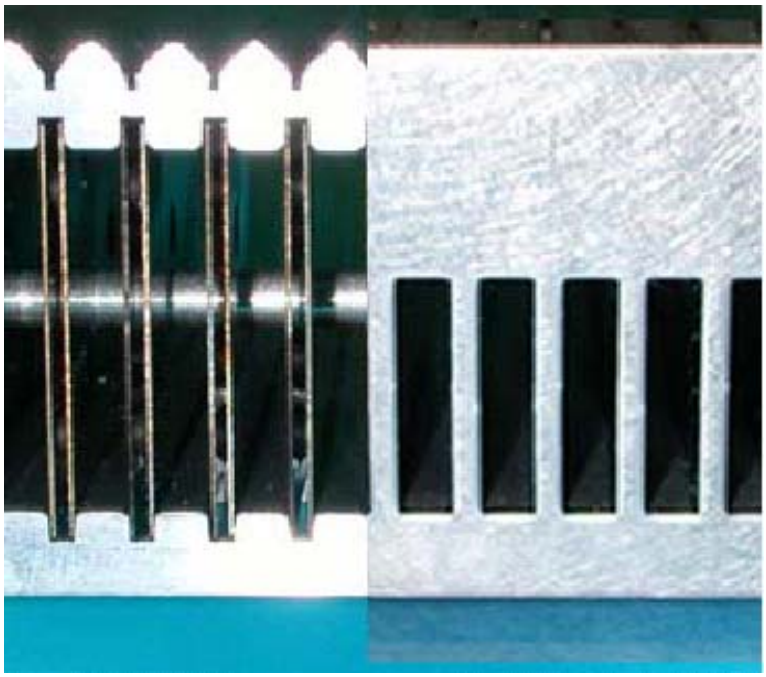

Figure 9

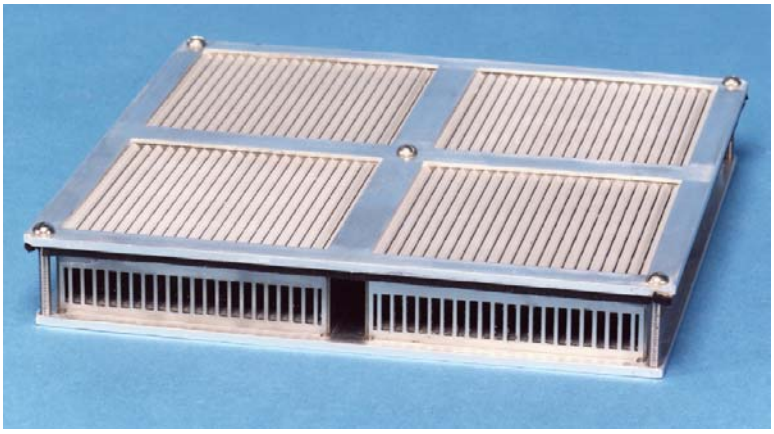

Figure 10

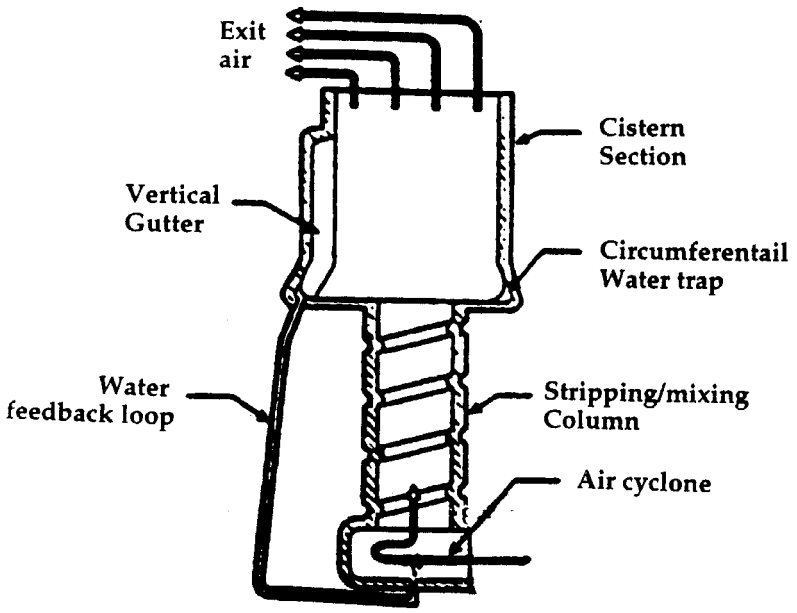
Exit
air
Cistern
Section
Vertical
Gutter
Circumferentail
Water trap
Water
feedback loop
Stripping/mixing
Column
Air cyclone

Figure 11.

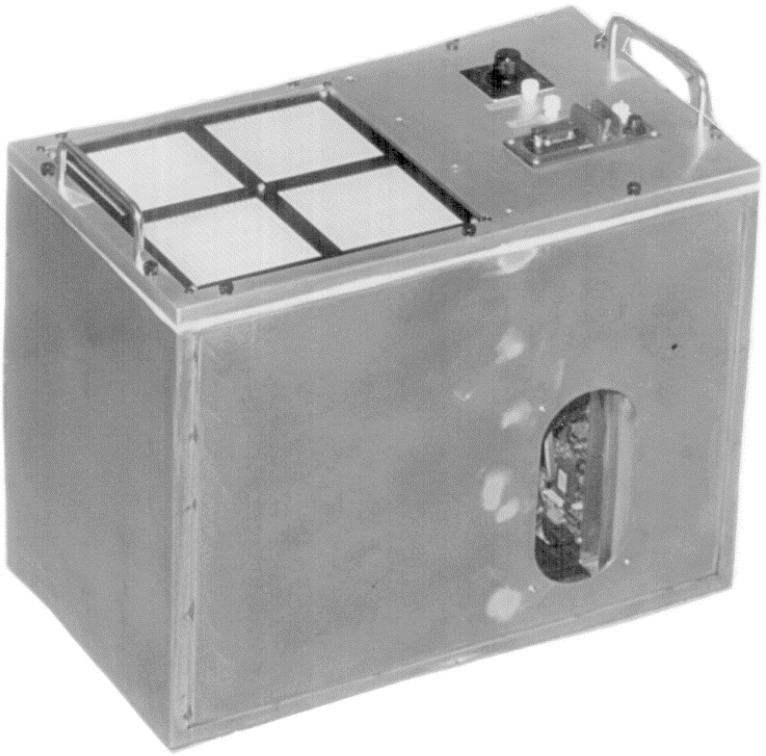

Figure 12

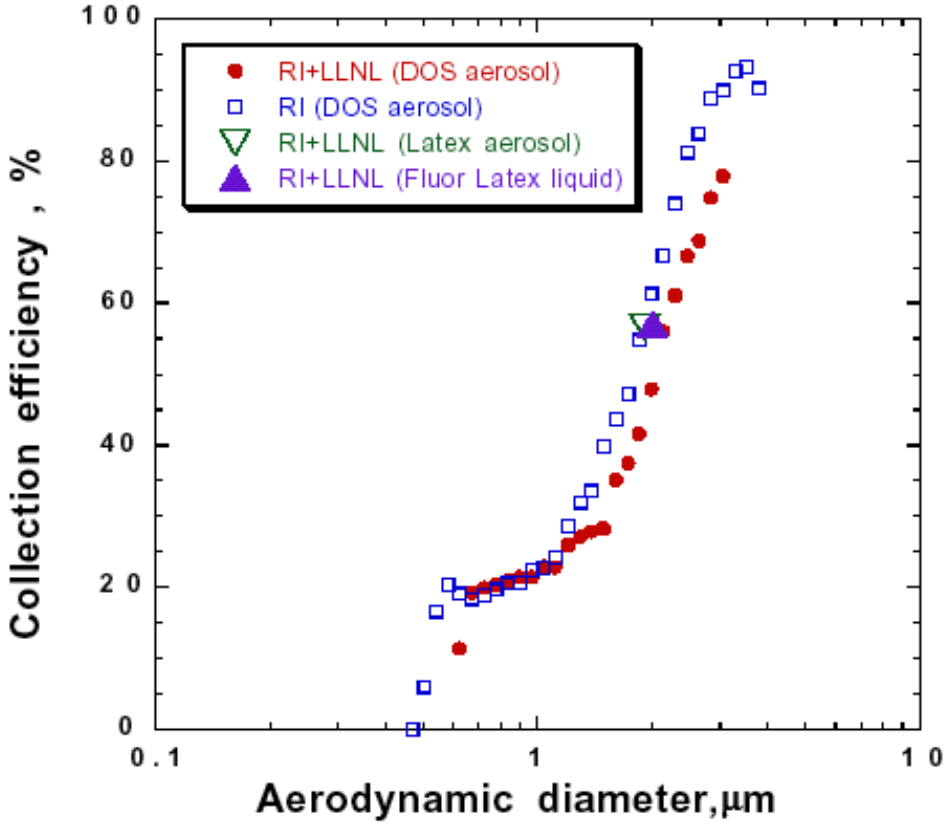
RI+LLNL (DOS aerosol)
RI (DOS aerosol)
RI+LLNL (Latex aerosol)
RI+LLNL (Fluor Latex liquid)
Collection efficiency , %
Aerodynamic diameter,µm
100
80
60
40
20
0
0.1
1
10

Figure 13

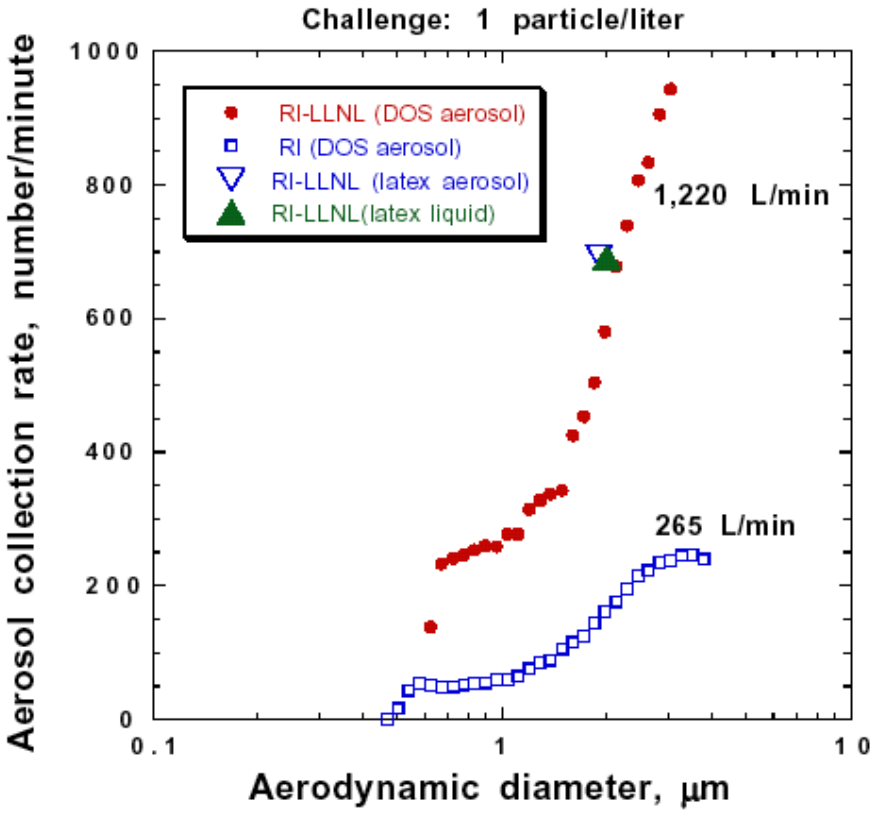
Challenge: 1 particle/liter
Aerosol collection rate, number/minute
1000
800
600
400
200
0
0.1
1
10
Aerodynamic diameter, µm
RI-LLNL (DOS aerosol)
RI (DOS aerosol)
RI-LLNL (latex aerosol)
RI-LLNL(latex liquid)
1,220 L/min
265 L/min

Figure 14

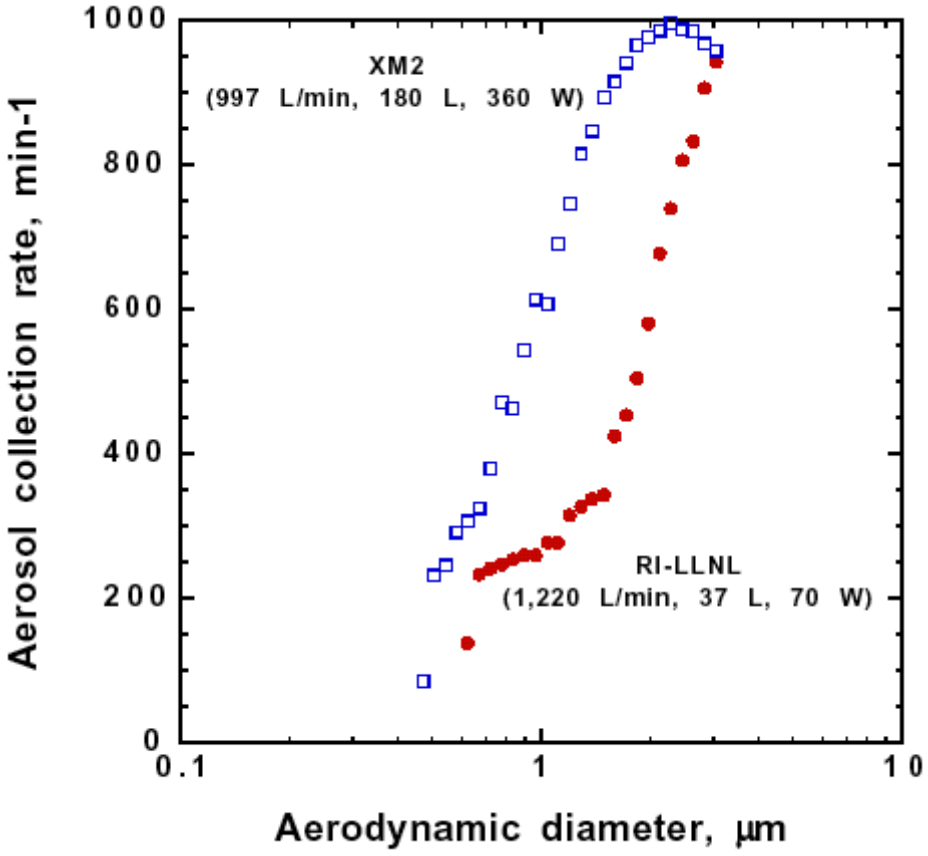
1000
800
600
400
200
0
0.1
1
10
Aerosol collection rate, min-1
Aerodynamic diameter, µm
XM2
(997 L/min, 180 L, 360 W)
RI-LLNL
(1,220 L/min, 37 L, 70 W)

Figure 15


LAWRENCE LIVERMORE NATIONAL LAB
APOLLO AEROSOL COLLECTOR

Figure 16

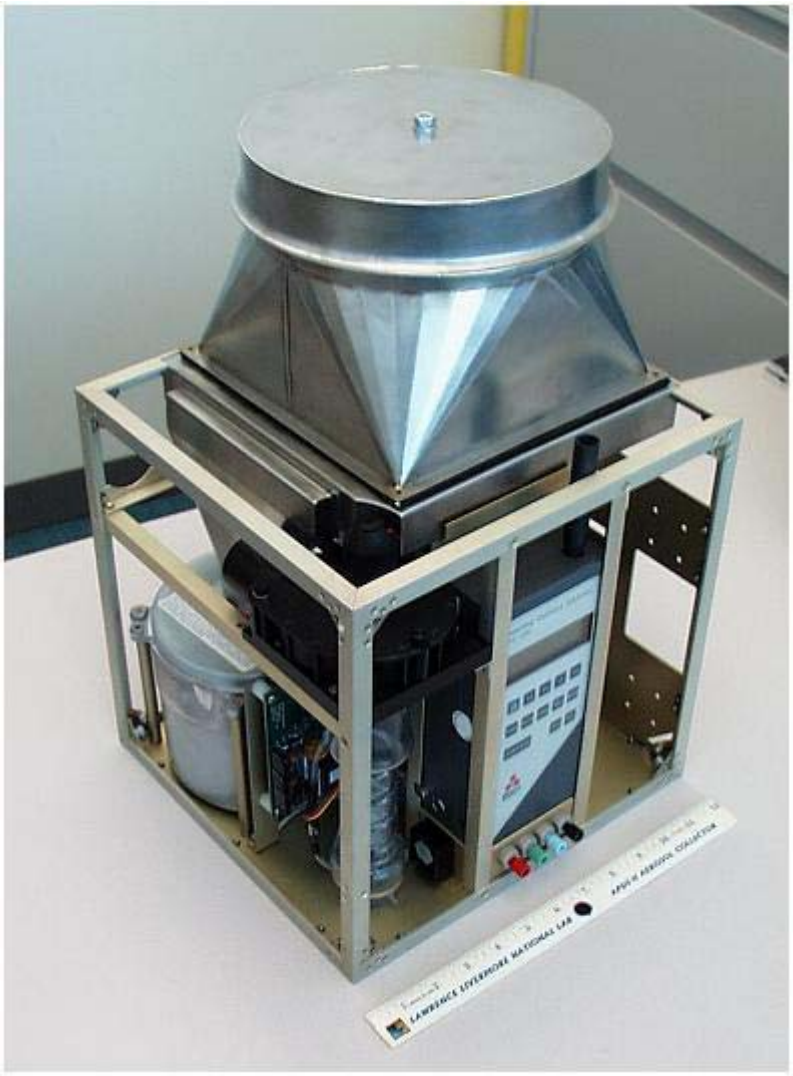

Figure 17.